



Temperature stability of individual plasmonic Au and TiN nanodiscs

RYAN BOWER,^{1,*}  CILLIAN P. T. MCPOLIN,^{2,3,4} ALEXEY V. KRASAVIN,² ANATOLY V. ZAYATS,² AND PETER K. PETROV¹

¹Department of Materials, Imperial College London, Royal School of Mines, Exhibition Road, London, SW7 2AZ, UK

²Department of Physics, King's College London, Strand, London, WC2R 2LS, UK

³Present address: Department of Chemistry, Molecular Sciences Research Hub, Imperial College London, White City, London W12 0BZ, UK

⁴c.mcpolin@imperial.ac.uk

*r.bower16@imperial.ac.uk

Abstract: Refractory plasmonic materials are of interest for high-temperature plasmonic applications due to their increased thermal stability when compared to gold and silver. Titanium nitride (TiN) has been highlighted as a promising refractory material, offering both strong plasmonic and thermal performance. In this work, we analyze the stability of both the structural and optical response of individual plasmonic nanodiscs of various diameters subjected to elevated temperature conditions in air. Using cathodoluminescence spectroscopy, we trace the resonance spectra and shape modifications of the same single TiN and Au discs annealed at increasing temperatures up to 325 °C. TiN discs display greater morphological stability, but the optical properties of both materials deteriorate from 200 °C, although the mechanisms of degradation are different. The results are essential for optimizing nanostructured materials for high temperature nanophotonic applications.

Published by Optica Publishing Group under the terms of the [Creative Commons Attribution 4.0 License](https://creativecommons.org/licenses/by/4.0/). Further distribution of this work must maintain attribution to the author(s) and the published article's title, journal citation, and DOI.

1. Introduction

Plasmonic research has enabled the realization of nanoscale optical components and continues to expand the range of applications for plasmonic materials and devices, which includes surface enhanced Raman spectroscopy, bio- and gas-sensing, optical waveguiding, catalysis and photodetection [1–6]. Plasmonic applications requiring high operational temperatures, such as nanotherapeutics, heat-assisted magnetic recording (HAMR), and thermophotovoltaics [7–10], are also of considerable interest. However, typical plasmonic materials such as gold and silver are unsuitable for such high temperature plasmonic applications, due to their poor thermal stability. Refractory plasmonic materials are therefore of increasing importance, presenting the potential to improve the performance and operational lifetimes of high temperature plasmonic devices.

Several studies have investigated refractory plasmonic materials, including traditional refractory metals, such as tungsten, niobium, and molybdenum, transition metal nitrides (TMN), and transition metal oxides [11–13]. Of the transition metal nitrides, titanium nitride (TiN) is of significant interest because of its high melting-point (2930 °C) and has thus been thoroughly studied. In addition to high thermal stability, it enables a spectrally tunable, relatively low loss optical response [14,15]. Although less efficient than gold in terms of optical losses and plasmon lifetimes, TiN has been highlighted as a promising material for thermoplasmonic applications [16]. Regarding its thermal stability, TiN thin films were reported to retain metallic behavior up to 1,200 °C in vacuum [17]. However, when annealed in air, substantial deterioration of the optical response was reported at temperatures above 500 °C as a result of oxidation. This is below

the temperature at which the optical response of gold thin films was reported to degrade, with morphological changes reported at temperatures of >600 °C [18]. The difference in degradation mechanism is noteworthy here, as changes in morphology become increasingly significant when materials are patterned on the nano- and micro-scale.

Indeed, just as the range of practical plasmonic applications has increased, so the scale of plasmonic devices continues to decrease. The consistent miniaturization of plasmonic devices has been facilitated by evermore sophisticated characterization methods and fabrication techniques, in addition to the ongoing exploration of new materials platforms [19]. Patterning and testing of alternative plasmonic materials, including refractory TMNs, has become more prevalent as it is essential to determine the suitability and limitations of thermoplasmonic materials when patterned on the nanoscale. In addition to the development of theoretical figures of merit for high temperature plasmonic applications [20,21], recent work has investigated the thermal stability of transition metal nitride arrays based on TiN and NbN [22]. Notably, the work of Gadalla et al. reported greater thermal stability of TiN nano-bowtie arrays compared to gold [23].

Whilst these previous reports investigate the plasmonic response and stability of plasmonic thin films and refractory nanoparticle arrays, to our knowledge, an assessment of the thermal stability of individual nanoparticles has not yet been completed. In previous studies of nanoparticle arrays the stability with temperature was assessed by averaging over an ensemble of many nanoparticles. In contrast, in this work we investigate the stability of individual nanodiscs and track the evolution of the optical and morphological changes of the same nanoparticle with temperature. Such an investigation of the stability of individual nanodiscs is made possible by our use of cathodoluminescence (CL) spectroscopy and is particularly relevant when considering applications that require discrete plasmonic components. For instance, HAMR heads typically utilize a plasmonic nanoparticle to focus light into a sub-wavelength region to locally heat a magnetic medium, and hence it is critical that it is thermally robust [9].

In this work, we investigate the temperature stability of nanostructured plasmonic materials at the level of individual nanodiscs, tracing both the shape modification and the optical response modification of the same nanostructure utilizing cathodoluminescence (CL) spectroscopy. In contrast to smooth plasmonic films, for which primarily the modification of the optical constants with annealing is important, for nanostructures, both morphology and optical constants can be modified at high temperatures. The electron beam of the CL microscope can be readily used to directly excite plasmonic modes with nanoscale resolution. Collection of the light emitted upon excitation can be used to identify plasmon resonances and hybrid modes, and also allows for the polarization and angular emission profile to be resolved [24,25]. This technique has successfully been used to measure emission from nanoantennas and individual metal nanoparticles [26–28].

Here, we compare the thermal stability of single nanoscale titanium nitride and gold discs, patterned on silicon substrates. Samples are annealed in air for 30 min each at temperatures ranging from 150 °C to 325 °C. Following each annealing stage, CL spectra and SEM images are collected to assess variations in the optical response and disc morphology. Experimental spectral data for the CL response of plasmonic discs are supplemented by simulations, identifying the excited plasmonic modes and confirming the oxidation-related mechanism of the change in the optical response of TiN nanodiscs with the annealing temperature.

2. Methods

2.1. Sample fabrication

Individual discs with diameters ranging from 150 nm to 450 nm and heights of 50 nm were patterned from gold and titanium nitride using electron beam lithography (EBL). Au and TiN nanodiscs measured in this study had diameters of 175, 220, 310 nm and 170, 260, 350 nm, respectively. Gold discs were prepared by thermal evaporation and patterned using a lift-off method. TiN discs were patterned using a reactive ion etching-based method [29,30]. A complete

description of the fabrication processes is included in the Supplementary Information. In brief, TiN nitride thin films (50 nm) are deposited by RF magnetron sputtering, coated with a Cr hard mask prepared via EBL patterning and lift-off, and then etched with chlorine based Reactive Ion Etching (RIE). The Cr mask is then removed with Cr etchant solution revealing the TiN nanodiscs.

2.2. Annealing study

A thermal annealing study was completed to assess the thermal stability of individual TiN discs in comparison with gold discs. For each material, SEM micrographs and CL spectra were initially collected for discs of comparable diameter using a Tescan-SEM Delmic-cathodoluminescence instrument. When collecting CL data, a 30 keV electron beam is rastered over an individual disc, exciting modes which subsequently radiate into the far-field. This emitted light is collected using a parabolic mirror and directed to a spectrometer and CCD camera. Substrate background emission is corrected for in the CL spectra, which are spatially averaged for each disc.

For the annealing study, the samples were then heated in air for 30 min before collecting further CL spectra and SEM images. Samples were sequentially heated at 100, 200, 300, and 325 °C. Following annealing, spectra and micrographs were collected from the same disc after each anneal, to ensure that any variations in the disc diameter and morphology arising from the fabrication process did not influence the spectra obtained. This also allows specific variations in the disc shape and spectra to be monitored. A schematic of the CL measurement process is included in Fig. 1. The spatial variation in the CL spectra is evident from Fig. 1(b), with further insight provided by simulations.

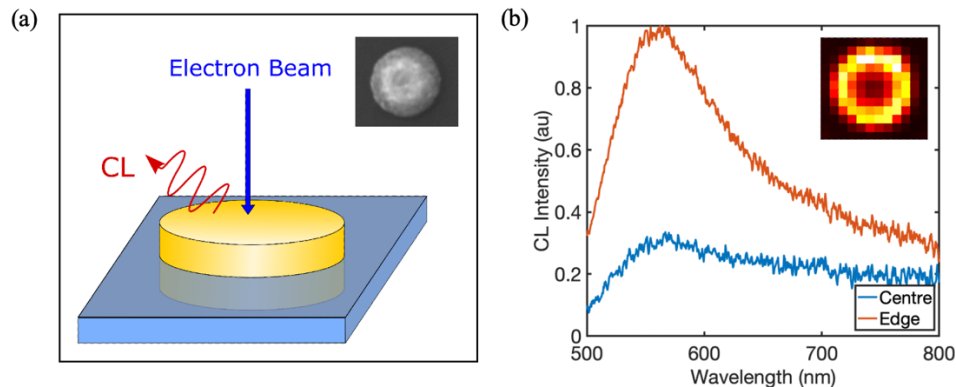


Fig. 1. Schematic of CL measurements. (a) E-beam irradiates the nanodiscs, with the resulting CL collected by a mirror and directed into a spectrometer. Inset: SEM image of an Au nanodisc (b) CL spectra, normalized to 1, for the e-beam placed at the edge (red line) and center (blue line) of an Au nanodisc (not annealed) with a diameter of 280 nm. Inset: Corresponding CL map at a wavelength of 580 nm.

2.3. Numerical simulations

Numerical modeling of the cathodoluminescence signal from Au and TiN nanodiscs was performed using a finite element method (COMSOL Multiphysics software). Generally, there are two mechanisms of cathodoluminescence, coherent and incoherent, but for plasmonic nanostructures, a coherent mechanism is dominant [31–33]. To model it, the CL source was implemented in simulations as a vertically-oriented point dipole at the nanodisc interface where the e-beam enters the structure, representing a collapsing dipole produced by the electron and its image charge. The dipole source was set to have a $1/\omega$ frequency dependence obtained from a

Fourier transform of the time-space trajectory of the moving electron in the beam. Five positions of the dipole along the nanodisc radius were studied, accounting for a CL signal from ring-shaped (or circular in the case of the central region) areas, altogether producing the overall measured signal (see Supplementary Information). The areas of these regions were set to be equal, while the position of the dipole inside each region was set in such a way that a circle passing through it divides the region into equal areal parts. The simulation domain was surrounded by perfectly matched layers to ensure the absence of back-reflection from the outer boundaries. The produced CL signal was integrated over a hemisphere surrounding the structure on the air side. The optical properties of Au, titanium oxynitride (TiON), and Si were taken from [34–36], respectively, while for TiN data collected using spectroscopic ellipsometry were used.

3. Results and discussion

3.1. Annealing study

Figure 2 displays the CL spectra of individual TiN and Au discs with respective diameters of 170, 220, 350 nm and 175, 260, 310 nm, collected throughout the annealing cycle. The cathodoluminescence spectra collected at room temperature (blue curves) display broad resonance peaks at ~550 nm for Au and at ~550-600 nm for TiN. The observation of TiN peaks at longer wavelengths than Au is expected as the plasmon resonances for TiN occurs at lower energy than Au, consistent with the literature [20,37,38]. This is further corroborated by spectroscopic ellipsometry measurements for TiN and Au thin films (Fig. S3.), in which the screened plasma energy for TiN thin films is observed at longer wavelength than those of Au. Additionally, the CL peaks for TiN peaks are broader than the Au peaks, which can be attributed to the higher losses.

SEM images of each disc, collected at RT and after each annealing step, are shown in the insets of Fig. 2 and in Figs. S4-S5. Upon inspection, it is observed that the gold discs of all diameters display obvious changes in structure and morphology from ~300 °C. The discs become deformed, likely due to melting and redistribution of the Au. The change of morphology in the Au nanoparticles is observed systematically in repeated experiments and is in agreement with the degradation mechanism previously reported for gold thin films, in which increased surface roughness results in film discontinuities. This increased surface roughness leads to greater scattering of the conduction electrons on the nanostructure surface and an increase in the magnitude of the imaginary dielectric permittivity, and, therefore, greater losses [39]. The previously reported deformation temperature for gold thin films in ambient conditions is 600 °C. Beyond this temperature the surface morphology of the films changes significantly, resulting in a loss of connectivity across the film and deterioration of the optical properties [18]. In contrast, the TiN discs retain their shape to 325 °C with no obvious changes in morphology or the disc shape. Indeed, TiN bowtie nanoantennas were previously reported to retain their shape when heated in air for 10 min at temperatures up to 800 °C with little change in microscopic appearance [23]. In a thin film form, TiN was reported to display a far less pronounced increase in roughness compared to gold when heated for one hour in air, so this lack of variation in surface morphology of the patterned discs is not unexpected [18].

Although the TiN discs do not display any deterioration in morphology or shape at elevated temperatures, there are significant changes in the CL spectra for both TiN and Au discs from 200 °C for all disc diameters measured (Fig. 2). For Au, we attribute this to changes in surface morphology observed in the SEM micrographs. However, in the TiN case, the spectral evolution is not due to morphological changes as evidenced by the SEM images. As the samples are annealed in air, it is likely that the degradation of the optical response arises from sample oxidation. This is consistent with the degradation mechanism previously reported for TiN thin films and TiN nanoparticle arrays, as discussed above. In our case, we see broadening of the out-of-plane resonant mode, as would be expected with a reduction in metallic character. The rate at which the plasmon peak broadens is dependent upon the extent of oxidation within the

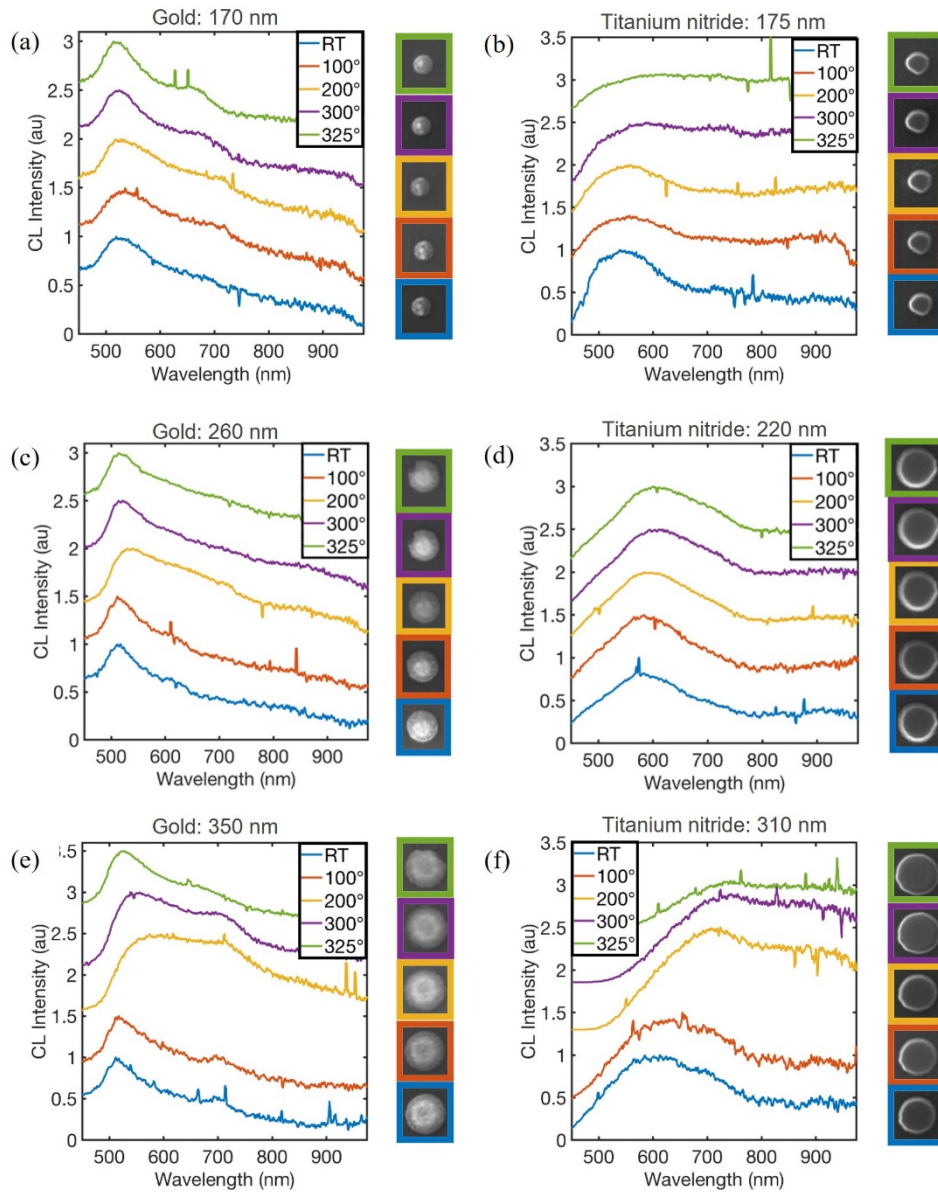


Fig. 2. Spatially averaged CL spectra and SEM images collected during the 30 min annealing study for (a,c,e) Au discs with diameters 170, 260 and 350 nm and (b,d,e) TiN discs with diameters 175, 220 and 310 nm. Each spectrum is normalized to 1 independently and vertically offset for visibility.

nanoparticles after annealing. For smaller TiN discs, the loss of the plasmon resonance peak at 325 °C is indicative of complete oxidation of the sample. Larger disc diameters retain some degree of plasmonic character at 325 °C, however, peak broadening and redshift of the resonant peaks in both the 220 nm and 350 nm TiN discs indicates significant oxidation of the samples.

3.2. Simulations

To understand the measured CL spectra, the mode profiles of Au and TiN nanodiscs were found performing numerical simulations with plane wave excitation for both s and p polarizations. This approach is more convenient, as in the direct simulation of the CL process the mode profiles are significantly disturbed by the point-like excitation source (see Methods). The obtained extinction spectra are presented in Fig. S9 in the Supplementary Information. The plasmonic mode observed in the CL experiments can be identified as an out-of-plane dipolar mode, which could be excited in the simulations only by the p -polarized illumination. The nature of the mode was additionally confirmed by plotting the corresponding charge maps on the surface of the nanodiscs (see insets, Fig. S9). In the case of TiN, the mode is red-shifted and broadened in comparison to Au, which agrees well with the experimentally observed CL results and indicates less metallic behavior of the material together with somewhat higher losses. In-plane resonant modes excited by s -polarized illumination found in the simulations are barely observed in the experimental CL spectra presumably due to a symmetry mismatch with the excitation CL source, which can be represented as vertically-polarized collapsing dipole.

After the identification of the peaks present in the CL spectrum, we proceeded with the modeling of the CL measurements themselves with a particular goal of checking the hypothesis that the modification of the spectrum with temperature in the case of TiN nanodiscs is related to their oxidation. Two possible scenarios of the oxidation process were considered. One is gradual expansion of a TiON 25% oxidized layer from the surface towards the nanodisc interior (which is assumed to be 10% oxidized already during the fabrication process), and another is uniform oxidation of the entire nanodisc characterized by the increase of the oxygen content from 10 to 40%. The results are presented in Fig. 3(a) and (b), respectively. Both oxidation models result in the red-shift and broadening of the plasmonic peak, correctly reproducing the experimental trends and thus supporting the oxidation-related interpretation of the change in the CL spectra with temperature. It can be logically assumed that the actual oxidation process is a cooperative action of the above model scenarios when the increase of the oxygen content and deeper penetration of oxygen atoms into the interior happen simultaneously.

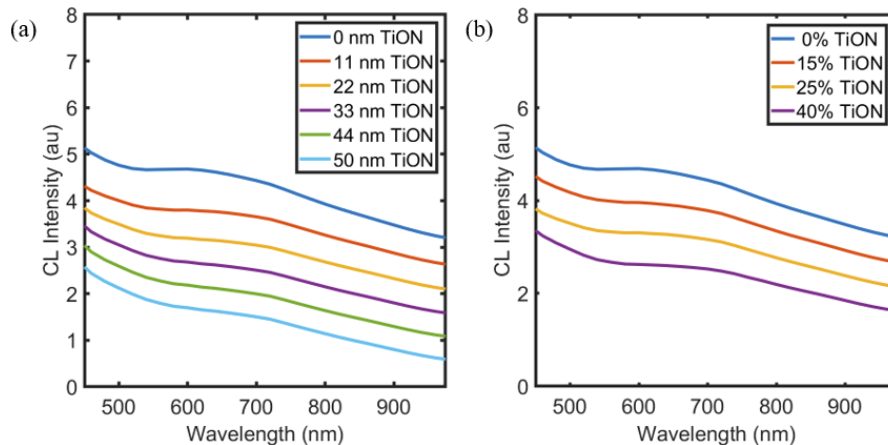


Fig. 3. Simulations of a coherent CL signal from (a) TiN/TiON core/shell disc, diameter 260 nm, with increasing TiON shell thickness and (b) TiON disc, diameter 260 nm, with increasing uniform oxidation of the disc. Spectra are vertically offset for visibility.

3.3. Discussion

From the experimental annealing study, we observe that TiN discs display greater morphological stability when compared to Au discs. However, both materials display deterioration of the optical properties and plasmonic response from 200 °C. Mechanistically, the optical degradation for Au and TiN is distinct, resulting from morphological changes and oxidation, respectively. This agrees with the previously reported degradation mechanism for Au and TiN plasmonic thin films. Additionally, this diminishment of the plasmonic character occurs at lower temperatures than reported for plasmonic thin films based on Au and TiN, which is expected for nano-patterned features due to the increased surface-volume ratio. Although the deterioration in plasmonic behavior reported here occurs at significantly lower temperatures than that of TiN nano-bowtie arrays (c.f. 200° and 600°C) [23], this can be explained by the significantly shorter annealing time of 10 min used in that work, compared to the 30 min anneal used here (see Supplementary Information). The degradation of optical properties at relatively low temperatures, therefore, indicates that plasmonic devices containing bare TiN nanoparticles are unsuitable for extended high-temperature operation in ambient conditions.

To overcome this, the application of small-scale TiN-based plasmonic components requires vacuum conditions, inert gas environments, or the use of an encapsulation layer to limit oxidation, as has previously been suggested [17,40,41]. However, similar encapsulation layers are also reported to improve the thermal stability of gold nanoparticles [42–44]. In this sense, the advantages of using TiN rather than gold are limited if both require a protective layer yet Au displays superior plasmonic properties, with lower loss and greater lifetimes. Nevertheless, the benefit of using encapsulated TiN rather than gold could arise from its spectral tunability and CMOS compatibility of the TMN. Additionally, TiN may be better suited than Au to specific plasmonic applications, such as local heating [20,29].

4. Conclusions

We have examined and reported the thermal stability of individual nanoscale TiN discs in comparison with gold. SEM imaging and CL spectroscopy indicate that although TiN displays superior thermal stability in comparison with Au when considering morphological changes and disc deformation, deterioration in the optical properties of both materials occurs at comparable temperatures. The degradation of individual discs occurs at significantly lower temperatures than previously reported for plasmonic thin films. From these results, it is apparent that oxidation of TMNs remains a limitation to the integration of TiN components within plasmonic devices to be used in ambient conditions. However, we suggest that TiN could display improved performance compared to gold when used in inert or vacuum environments or when coated with an optically transparent protective layer, particularly when used for targeted plasmonic applications such as local heat generation.

Funding. European Research Council (789340); Engineering and Physical Sciences Research Council (EP/L015277/1, EP/M013812/1, EP/P02520X/1, EP/R00661X/1, EP/V001914/).

Disclosures. The authors declare no conflicts of interest.

Data availability. All the data supporting this research are presented in the results section and supplementary materials and are available from the corresponding authors upon reasonable request.

Supplemental document. See [Supplement 1](#) for supporting content.

References

1. B. Sharma, R. R. Frontiera, A.-I. Henry, E. Ringe, and R. P. Van Duyne, “SERS: Materials, applications, and the future,” *Mater. Today* **15**(1-2), 16–25 (2012).
2. F. Xie, J. S. Pang, A. Centeno, M. P. Ryan, D. J. Riley, and N. M. Alford, “Nanoscale control of Ag nanostructures for plasmonic fluorescence enhancement of near-infrared dyes,” *Nano Res.* **6**(7), 496–510 (2013).
3. M. E. Nasir, W. Dickson, G. A. Wurtz, W. P. Wardley, and A. V. Zayats, “Hydrogen detected by the naked eye: optical hydrogen gas sensors based on core/shell plasmonic nanorod metamaterials,” *Adv. Mater.* **26**(21), 3532–3537 (2014).

4. M. Sistani, M. G. Bartmann, N. A. Güsken, R. F. Oulton, H. Keshmiri, M. S. Seifner, S. Barth, N. Fukata, M. A. Luong, M. I. D. Hertog, and A. Lugstein, "Nanoscale aluminum plasmonic waveguide with monolithically integrated germanium detector," *Appl. Phys. Lett.* **115**(16), 161107 (2019).
5. Z. Zhang, C. Zhang, H. Zheng, and H. Xu, "Plasmon-driven catalysis on molecules and nanomaterials," *Acc. Chem. Res.* **52**(9), 2506–2515 (2019).
6. N. A. Güsken, A. Lauri, Y. Li, T. Matsui, B. Doiron, R. Bower, A. Regoutz, A. Mihai, P. K. Petrov, R. F. Oulton, L. F. Cohen, and S. A. Maier, "TiO₂-x-enhanced ir hot carrier based photodetection in metal thin film–Si junctions," *ACS Photonics* **6**(4), 953–960 (2019).
7. X. Huang and M. A. El-Sayed, "Plasmonic photo-thermal therapy (PPTT)," *Alexandria J. Med.* **47**(1), 1–9 (2011).
8. V. P. Zharov, K. E. Mercer, E. N. Galitovskaya, and M. S. Smeltzer, "Photothermal nanotherapeutics and nanodiagnostics for selective killing of bacteria targeted with gold nanoparticles," *Biophys J* **90**(2), 619–627 (2006).
9. N. Zhou, X. Xu, A. T. Hammack, B. C. Stipe, K. Gao, W. Scholz, and E. C. Gage, "Plasmonic near-field transducer for heat-assisted magnetic recording," *Nanophotonics* **3**(3), 141–155 (2014).
10. C. Wu, B. Neuner Iii, J. John, A. Milder, B. Zollars, S. Savoy, and G. Shvets, "Metamaterial-based integrated plasmonic absorber/emitter for solar thermo-photovoltaic systems," *J. Opt.* **14**(2), 024005 (2012).
11. A. Banerjee, R. M. Heath, D. Morozov, D. Hemakumara, U. Nasti, I. Thayne, and R. H. Hadfield, "Optical properties of refractory metal based thin films," *Opt. Mater. Express* **8**(8), 2072–2088 (2018).
12. M. P. Wells, B. Zou, A. P. Mihai, R. Bower, B. Doiron, A. Regoutz, S. Fearn, S. A. Maier, N. M. Alford, and P. K. Petrov, "Multiphase strontium molybdate thin films for plasmonic local heating applications," *Opt. Mater. Express* **8**(7), 1806–1817 (2018).
13. U. Guler, A. V. Kildishev, A. Boltasseva, and V. M. Shalaev, "Plasmonics on the slope of enlightenment: the role of transition metal nitrides," *Faraday Discuss.* **178**, 71–86 (2015).
14. G. V. Naik, J. Kim, and A. Boltasseva, "Oxides and nitrides as alternative plasmonic materials in the optical range [Invited]," *Opt. Mater. Express* **1**(6), 1090–1099 (2011).
15. P. Patsalas, N. Kalfagiannis, and S. Kassavetis, "Optical properties and plasmonic performance of titanium nitride," *Materials* **8**(6), 3128–3154 (2015).
16. A. Lalisse, G. Tessier, J. Plain, and G. Baffou, "Plasmonic efficiencies of nanoparticles made of metal nitrides (TiN, ZrN) compared with gold," *Sci. Rep.* **6**(1), 38647 (2016).
17. J. A. Briggs, G. V. Naik, Y. Zhao, T. A. Petach, K. Sahasrabudhe, D. Goldhaber-Gordon, N. A. Melosh, and J. A. Dionne, "Temperature-dependent optical properties of titanium nitride," *Appl. Phys. Lett.* **110**(10), 101901 (2017).
18. M. P. Wells, R. Bower, R. Kilmurray, B. Zou, A. P. Mihai, G. Gobalakrishnan, N. M. Alford, R. F. M. Oulton, L. F. Cohen, S. A. Maier, A. V. Zayats, and P. K. Petrov, "Temperature stability of thin film refractory plasmonic materials," *Opt. Express* **26**(12), 15726–15744 (2018).
19. M. I. Stockman, K. Kneipp, S. I. Bozhevolnyi, S. Saha, A. Dutta, J. Ndukaife, N. Kinsey, H. Reddy, U. Guler, V. M. Shalaev, A. Boltasseva, B. Gholipour, H. N. S. Krishnamoorthy, K. F. MacDonald, C. Soci, N. I. Zheludev, V. Savinov, R. Singh, P. Groß, C. Lienau, M. Vadai, M. L. Solomon, D. R. Barton, M. Lawrence, J. A. Dionne, S. V. Boriskina, R. Esteban, J. Aizpurua, X. Zhang, S. Yang, D. Wang, W. Wang, T. W. Odom, N. Accanto, P. M. D. Roque, I. M. Hancu, L. Piatkowski, N. F. V. Hulst, and M. F. Kling, "Roadmap on plasmonics," *Journal of Optics* **20**(4), 043001 (2018).
20. B. Doiron, M. Mota, M. P. Wells, R. Bower, A. Mihai, Y. Li, L. F. Cohen, N. M. Alford, P. K. Petrov, R. F. Oulton, and S. A. Maier, "Quantifying figures of merit for localized surface plasmon resonance applications: a materials survey," *ACS Photonics* **6**(2), 240–259 (2019).
21. A. Lalisse, G. Tessier, J. Plain, and G. Baffou, "Quantifying the efficiency of plasmonic materials for near-field enhancement and photothermal conversion," *J. Phys. Chem. C* **119**(45), 25518–25528 (2015).
22. P. Karl, M. Ubl, M. Hentschel, P. Flad, Z.-Y. Chiao, J.-W. Yang, Y.-J. Lu, and H. Giessen, "Optical properties of niobium nitride plasmonic nanoantennas for the near- and mid-infrared spectral range," *Opt. Mater. Express* **10**(10), 2597–2606 (2020).
23. M. N. Gadalla, A. S. Greenspon, M. Tamagnone, F. Capasso, and E. L. Hu, "Excitation of strong localized surface plasmon resonances in highly metallic titanium nitride nano-antennas for stable performance at elevated temperatures," *ACS Appl. Nano Mater.* **2**(6), 3444–3452 (2019).
24. E. J. R. Vesseur, J. Aizpurua, T. Coenen, A. Reyes-Coronado, P. E. Batson, and A. Polman, "Plasmonic excitation and manipulation with an electron beam," *MRS Bull.* **37**(8), 752–760 (2012).
25. T. Coenen and N. M. Haegel, "Cathodoluminescence for the 21st century: Learning more from light," *Appl. Phys. Rev.* **4**(3), 031103 (2017).
26. "Imaging electric and magnetic modes and their hybridization in single and dimer AlGaAs nanoantennas," (2021).
27. T. Coenen, E. J. R. Vesseur, A. Polman, and A. F. Koenderink, "Directional emission from plasmonic Yagi–Uda antennas probed by angle-resolved cathodoluminescence spectroscopy," *Nano Lett.* **11**(9), 3779–3784 (2011).
28. T. Coenen, F. Bernal Arango, A. Femius Koenderink, and A. Polman, "Directional emission from a single plasmonic scatterer," *Nat. Commun.* **5**(1), 3250 (2014).
29. U. Guler, J. C. Ndukaife, G. V. Naik, A. G. A. Nnanna, A. V. Kildishev, V. M. Shalaev, and A. Boltasseva, "Local Heating with Lithographically Fabricated Plasmonic Titanium Nitride Nanoparticles," *Nano Lett.* **13**(12), 6078–6083 (2013).
30. J. A. Briggs, G. V. Naik, T. A. Petach, B. K. Baum, D. Goldhaber-Gordon, and J. A. Dionne, "Fully CMOS-compatible titanium nitride nanoantennas," *Appl. Phys. Lett.* **108**(5), 051110 (2016).

31. C. P. , H. Kh, A. F. Kh, Kh , M. Je, and F. Nx, "Imaging of plasmonic modes of silver nanoparticles using high-resolution cathodoluminescence spectroscopy," *ACS Nano* **3**(1), 1 (2009).
32. F. J. García de Abajo, "Optical excitations in electron microscopy," *Rev. Mod. Phys.* **82**(1), 209–275 (2010).
33. P. Das and T. K. Chini, "Spectroscopy and imaging of plasmonic modes over a single decahedron gold nanoparticle: a combined experimental and numerical study," *J. Phys. Chem. C* **116**(49), 25969–25976 (2012).
34. R. W. Johnson and P. B. Christy, "Optical Constants of the Noble Metals," *Phys. Rev. B* **6**, 4370 (1972).
35. B. Doiron, Y. Li, A. Mihai, S. D. Forno, S. Fearn, L. F. Cohen, N. M. Alford, J. Lischner, P. Petrov, S. A. Maier, and R. F. Oulton, "Optimizing hot electron harvesting at planar metal-semiconductor interfaces with titanium oxynitride thin films," (2018).
36. C. Schinke, P. Christian Peest, J. Schmidt, R. Brendel, K. Bothe, M. R. Vogt, I. Kröger, S. Winter, A. Schirmacher, S. Lim, H. T. Nguyen, and D. MacDonald, "Uncertainty analysis for the coefficient of band-to-band absorption of crystalline silicon," *AIP Adv.* **5**(6), 067168 (2015).
37. G. V. Naik, J. L. Schroeder, X. J. Ni, A. V. Kildishev, T. D. Sands, and A. Boltasseva, "Titanium nitride as a plasmonic material for visible and near-infrared wavelengths," *Opt. Mater. Express* **2**(4), 478–489 (2012).
38. G. V. Naik, V. M. Shalaev, and A. Boltasseva, "Alternative plasmonic materials: beyond gold and silver," *Adv. Mater.* **25**(24), 3264–3294 (2013).
39. H. Reddy, U. Guler, A. V. Kildishev, A. Boltasseva, and V. M. Shalaev, "Temperature-dependent optical properties of gold thin films," *Opt. Mater. Express* **6**(9), 2776–2802 (2016).
40. S. Bagheri, C. M. Zgrabik, T. Gissibl, A. Tittl, F. Sterl, R. Walter, S. De Zuani, A. Berrier, T. Stauden, G. Richter, E. L. Hu, and H. Giessen, "Large-area fabrication of TiN nanoantenna arrays for refractory plasmonics in the mid-infrared by femtosecond direct laser writing and interference lithography [Invited]," *Opt. Mater. Express* **5**(11), 2625–2633 (2015).
41. W. Li, U. Guler, N. Kinsey, G. V. Naik, A. Boltasseva, J. Guan, V. M. Shalaev, and A. V. Kildishev, "Refractory plasmonics with titanium nitride: broadband metamaterial absorber," *Adv. Mater.* **26**(47), 7959–7965 (2014).
42. G. Albrecht, S. Kaiser, H. Giessen, and M. Hentschel, "Refractory plasmonics without refractory materials," *Nano Lett.* **17**(10), 6402–6408 (2017).
43. Y.-S. Chen, W. Frey, S. Kim, K. Homan, P. Kruizinga, K. Sokolov, and S. Emelianov, "Enhanced thermal stability of silica-coated gold nanorods for photoacoustic imaging and image-guided therapy," *Opt. Express* **18**(9), 8867–8878 (2010).
44. C. Radloff and N. J. Halas, "Enhanced thermal stability of silica-encapsulated metal nanoshells," *Appl. Phys. Lett.* **79**(5), 674–676 (2001).